Laser and Particle Beams (2001), *19*, 443–449. Printed in the USA.

Precursor phenomenon in wire arrays: Model and experiment

R.B. BAKSHT, V.I. KOKSHENEV, AND N.A. RATAKHIN
High Current Electronics Institute, SB RAS, Tomsk, 634055, Russia
(RECEIVED 22 May 2000; ACCEPTED 31 March 2001)

1. INTRODUCTION

To understand in detail what happens with an imploding wire array would require one to account for many different processes beginning with the wire explosion and ending with the Rayleigh–Taylor instabilities. Haines (1998) has performed a heuristic analysis of the multiwire array implosion and suggested that the dynamics and behavior of the wire array pinch be divided into four distinct phases. These phases are as follows: the electrical explosion of an individual wire (Phase 1), merging of the wire plasmas and the current shell formation (Phase 2), running-in of the wire array (Phase 3), and the stagnation of the pinch at the axis (Phase 4).

In this paper we discuss some details inherent in Phase 3, namely, the problem of the appearance and development of a precursor. The precursor appearance in an imploding *z* pinch is possible if the plasma skin layer is absent and the conductivity of the inner layers of the plasma shell rises more rapidly than the conductivity of the outer layers. The precursor is related to the light plasma flows that are accelerated inward toward the wire array axis before the main mass of the imploded wires starts moving. The appearance of a precursor in the wire arrays was observed in earlier experiments of Aivazov *et al.* (1987) and Baksht *et al.* (1989). Lebedev *et al.* (1998) studied the formation of a precursor and has shown that the precursor mass can make up a few percent of the wire array mass. As noted below, the precursor current can be 20–30% of the total current of the wire array. This phenomenon alone impairs the implosion dynamics. Besides, even small quantities of hot plasma on the axis preclude high compression ratios and reduce the efficiency of the conversion of the electrical energy into radiation.

The reason for the precursor appearance is related to the peculiarities of the wire explosion in vacuum. For a wire current density rate of rise typical for wire array experiments, 10^{17} A/cm^2-s, the outer layer of the wire expands and forms a high-conductivity plasma corona (Baksht *et al.*, 1983; Zakharov *et al.*, 1983). As a result, the plasma of an individual wire represents a heterogeneous pinch in which the core density should be a few orders of magnitude higher than the corona density (Ratachin & Baksht, 2001). The corona temperature, on the contrary, should be a few orders of magnitude higher than the core temperature. After the merging of the heterogeneous wire plasmas, a nonuniform plasma shell appears.

In this shell, segments with high temperature and low density alternate with segments with low temperature and high density. Naturally, this has a beneficial effect on the precursor formation. In the present paper, we develop the precursor phenomenon model and compare the theoretical results with the experimental data. The paper is structured as follows. In Section 2, we present analytical formulae on the dependencies of the precursor current on the wire-array rise time and the wire array parameters. In Section 3, the theoretical estimates are compared to experimental data for nanosecond and microsecond modes of wire array implosions. In Section 4, we conclude with a discussion.

2. PRECURSOR DUE TO HIGH RESISTANCE WIRE CORE

The idea of the model is as follows: Let us imagine that after the merging of the wire plasmas, two current shells will

Address correspondence and reprint requests to: R.B. Baksht, High Current Electronics Institute, SB RAS, Tomsk, 634055, Russia. E-mail: vikhrev@nfi.kiae.ru

Editor's Note: Due to communication difficulties, the proof copy for this article was not reviewed by the authors. Every effort has been made to eliminate errors, but the publisher cannot assume responsibility for the accuracy of this article.

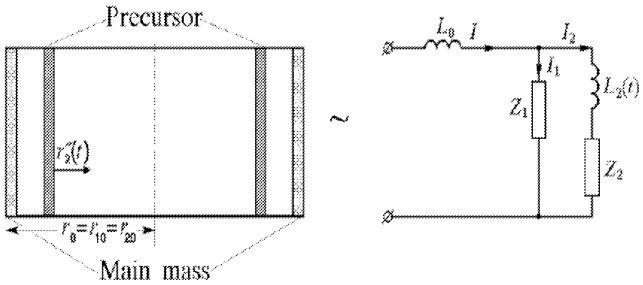

Fig. 1. Sketch of the precursor shell and the main mass shell, and an equivalent circuit diagram for the implosion of these shells. I is the wire-array total current; I_1 and I_2 are the currents of the main mass shell and the precursor shell, respectively.

exist: current shell **I** with mass per unit length m_1 and current I_1 and current shell **II** with mass per unit length m_2 and current I_2. The mass m_1 is equal to the net mass of the cores of the individual wires and mass m_2 is equal to the net mass of the coronas of the individual wires.

The mass m_2 is much lower than the mass m_1. We assume that as the current starts flowing, only current shell **II** will move. Usually the principal circuit includes the mutual and the self-inductance of the loops. For the cylindrical case, the circuit can be simplified as shown in Figure 1. In Figure 1 L_0 is the inductance of the loop which is formed by the shell **I** and the external current posts. L_2 is the inductance of the loop which is formed by the shell **I** and the moving shell **II**. The total current through the wire array can be presented as

$$I = I_1 + I_2 = bt, \tag{1}$$

where b is equal to I_m/t_r with I_m being the total current amplitude and t_r the total current rise time. For the initial shell radius, we have $r_{10} = r_{20} = r_0$, where r_0 is the initial radius of the wire array. For the currents I_1 and I_2, in view of the circuit given in Figure 1, we then have the equation

$$\frac{d(I_2 L_2)}{dt} + I_2(z_2 + z_1) = Iz_1, \tag{2}$$

where z_1 and z_2 are the resistance of shell **I** and shell **II**, respectively, and $dL_1/dt = 0$, as the main part of the wire array is stationary.

The inductance L_2 is related to the radius $r_2(t)$ as

$$L_2 = \frac{\mu_0}{2\pi} \ln \frac{r_0}{r_2(t)} = \frac{\mu_0}{2\pi} \ln \frac{1}{1-x}, \tag{3}$$

where $x(t)$, the distance for which the light current shell II moves inward, is given by

$$x(t) = [r_0 - r_2(t)]/r_0.$$

Let us consider the behavior of the terms in the left-hand side of Eq. (2). The first term is zero up to the time when the precursor starts moving. The currents in the first and second shells are in inverse proportion to the shell resistance before the precursor formation. In the general case, the resistance of an imploding pinch is determined by the Spitzer conductivity formula and the typical value of the resistance is 0.0075 Ω/cm for a 1-cm radius hollow pinch with a 0.5-cm shell thickness and an electron temperature equal to 2 eV. The impedance, inversely related to the inductance L_2, increases after the onset of the motion of shell **II** corresponding to the appearance of the precursor. With the typical velocity of motion of the precursor $v_{pr} = 1.5 \times 10^7$ cm/s and $x = 0.5$ we have for a 1-cm radius imploding pinch $L_2' = 2 \times 10^{-9} v_{pr}/r_2(t) = 0.06\ \Omega$/cm. This impedance is much greater than the Spitzer resistance estimated above. It follows that, first, the resistance related to the "immobile" portion of an imploding multiwire array is one or two orders of magnitude higher than the Spitzer resistance. Otherwise the precursor current would be shunted as early as at $x = 0.05$ owing to the high conductivity of shell **I**. Second, for $x \to 1$ we have $L_2' \to \infty$. This implies that the current through the precursor will disappear as soon as $z_2 + z_1$ becomes smaller than L_2'. In other words, the precursor current will have a maximum I_{2m}. The precursor current is equal to I_{2m} at the point in time labeled t_m (Fig. 2).

To find the relation between the precursor current and the implosion parameters, we should use, besides the circuit equation, the equation of motion for the imploding precursor mass

$$m_2 x''(t) = -\mu_0 I_2^2(t)/(4\pi r_2). \tag{4}$$

In dimensionless form, Eqs. (2) and (4) will appear as:

$$\alpha \frac{d}{d\tau}\left[i_2 \ln \frac{1}{1-x}\right] + i_2 = \tau, \tag{5}$$

$$x''(1-x) = \beta i_2^2, \tag{6}$$

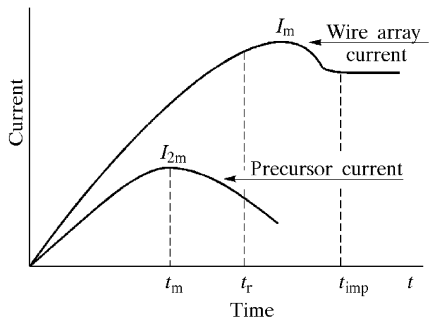

Fig. 2. Current waveforms for the wire array and for the precursor. I_{2m} is the maximum precursor current and I_m is the maximum wire array total current.

https://doi.org/10.1017/S026303460119302X Published online by Cambridge University Press

where

$$\alpha = \frac{\mu_0}{2\pi}\frac{1}{t_r(z_1+z_2)},$$

$$\beta = \frac{\mu_0}{4\pi}\frac{I_{2m}^2 z_1^2 t_r^2}{r_0^2 m_2 (z_1+z_2)^2},$$

$$\tau = \frac{t}{t_r}, \qquad i_2 = \frac{I_2}{I_m}\frac{z_1+z_2}{z_1},$$

$$x|_{t=0} = x'|_{t=0} = 0.$$

It can be shown that for small values of α we have

$$x = \frac{\beta\tau^4}{12}\left(1+\frac{3}{14}\frac{\beta\tau^4}{12}\right) = x_0\left(1+\frac{3}{14}x_0\right); \tag{7}$$

$$x' \approx 0.85\sqrt{2\beta i_{2m}^2 \ln[(1-x)^{-1}]}. \tag{8}$$

The quantity $x_0 = \beta\tau^4/12$ is the first approximation for x, and this approximation is operative at times $\tau \le \tau_m$. To find the precursor current, we rewrite Eq. (5) in a more convenient form:

$$i_2 = \frac{\tau - \alpha i_2' \ln(1-x)^{-1}}{1+\alpha x'/(1-x)} = \tau\frac{1-(\alpha\tau)i_2'\ln(1-x)^{-1}}{1+\alpha x'(1-x)}. \tag{9}$$

We have shown that, the limit of the precursor current is mainly associated with the increase of the term $\alpha x'/(1-x)$ in expression (9).

Moreover, we have $i_2' = 0$ for $i_2 = i_{2m}$ and so may neglect the second term in the numerator of Eq. (9) and write for i_2 at the point of its maximum

$$i_2 \approx \tau(1-x)/(1-x+\alpha x'). \tag{10}$$

Putting $x = x_0$, we may find with a low error (up to 10%) the current dependence $i_2 = f(\tau)$ in the neighborhood of the point τ_m:

$$i_2 = \frac{\tau(1-x_0)}{1-x_0+4\alpha(\beta/12)^{1/4}x_0^{3/4}}. \tag{11}$$

The condition $i_2' = 0$, $i_2'' < 0$ allows us to find the time τ_m at which the current reaches its maximum using the formula

$$\mu x_m^{3/4}(1+x_m) + x_m(2-x_m) = 1, \tag{12}$$

where

$$\mu = 8\alpha\beta/12, \qquad x_m = x_0|_{\tau=\tau_m} = \beta\tau_m^4/12.$$

Finding μ from Eq. (12) and substituting the value found into Eq. (11), we obtain

$$\mu = (1-x_m)^2/[x_m^{3/4}(1+x_m)], \tag{13}$$

$$i_{2m} = 2\tau_m(1+x_m)/(3+x_m). \tag{14}$$

Solving Eqs. (13) and (14) in view of Eq. (12) for specific values of x_m and μ, entirely determined by the wire array parameters we may find the maximum precursor current. This allows us to determine the energy ϵ lost with the appearance of the precursor.

Let us return to Eqs. (5) and (6) and recollect that the first term in Eq. (5) is in fact the differential of the magnetic flux Φ_2 associated with the moving plasma of the precursor:

$$i_2\alpha\ln(1-x)^{-1} = i_2 L_2 = \Phi_2.$$

The equation of motion, Eq. (6), in view of the above reasoning can be rewritten so that the acceleration is a function of the magnetic flux Φ_2:

$$x'' = \beta\frac{\Phi_2}{L_2}\frac{i_2}{1-x}. \tag{15}$$

Multiplication of Eq. (15) by x' and integration of the resulting equation yields

$$\epsilon_2 = \frac{x'^2}{2} = \frac{x_m'^2}{2} + \int_{\tau_m}^{\tau}\beta\Phi_2 i_2\frac{x'}{(1-x)L_2}\,d\tau$$

$$= \frac{x_m'^2}{2} + \int_{\tau_m}^{\tau}\beta\Phi_2 i_2\frac{dL_2}{L_2}, \tag{16}$$

where ϵ_2 is the energy of the precursor and $x_m'^2/2$ is its kinetic energy at $\tau = \tau_m$. For $i_2 = \tau$ we can find this energy from Eq. (5):

$$\frac{x_m'^2}{2} = \frac{\alpha i_{2m}^2}{2}\ln\frac{1}{1-x_m}.$$

In expression (16), the integral in the right part is equal to the work done by the magnetic field after the instant the current through the precursor has begun to fall. Let us show that this is the case. The energy of a imploding cylindrical shell being compressed by its self current i can be written for the time $\tau > \tau_m$ as

$$W_B = \int i^2\,dL = \int\frac{i\Phi}{L}\,dL = \langle i\Phi\rangle\ln\frac{L_f}{L_m}, \tag{17}$$

where W_B is the energy of the magnetic field associated with the moving shell and L_f is the pinch inductance at the final

https://doi.org/10.1017/S026303460119302X Published online by Cambridge University Press

compression. If the moving shell goes on moving once the current has reached its peak, the total energy W_B remains, in fact, unchanged. Only the density of this energy changes due to an increase in the volume taken by the magnetic field. The time-averaged quantity $\langle i\Phi \rangle$ is equal with good accuracy to $\langle i_m \Phi_m \rangle$, where the subscription m, as earlier, refers to the point where the current peaks. Then we have for ϵ_2

$$\epsilon_2 = \frac{x_m'^2}{2} + \int_{\tau_m}^{\tau} \frac{i_2 \Phi_2}{L}\, dL = \frac{x_m'^2}{2} + \langle i_2 \Phi_2 \rangle \ln \frac{L_f}{L_m}. \tag{18}$$

The final expression for ϵ_2 is as follows:

$$\epsilon_2 = \left[\frac{\alpha i_{2m}^2}{2} \ln \frac{1}{1 - x_m} \right] \left(1 + \ln \frac{L_f}{L_m} \right). \tag{19}$$

Using expressions (13)–(14) we can find the dependencies of the maximum precursor current and of the precursor energy on the parameters α and β. Note that the formula for β can be rewritten as

$$\beta = k[z_1^2/(z_1 + z_2)^2](M/m_2), \tag{20}$$

where

$$M = \frac{1}{k} \frac{\mu_0}{4\pi} \frac{I^2 t_{imp}^2}{r_0^2}$$

is the wire array mass calculated by the zero-dimensional model; k is a numerical factor equal to 8.4 for $I = I_m t/t_r$ and $t_{imp} = t_r$ and 2 for $I = I_m \sin \omega t$ and $t_{imp} = 1.1\pi/(2\omega)$. Thus, the value of β is mainly determined by the precursor mass. According to Ratachin & Baksht (2001), the ratio m_2/M makes up a few percent, and, hence, the actual range of β values is comparatively narrow. From Eq. (20) it can be inferred that for $z_1 > z_2$, the range of β values is 20–200, which corresponds to 1–10% of the mass going away. Dependence of the precursor current on the parameter $\alpha = \mu_0/[2\pi t_r(z_1 + z_2)]$ is shown in Figure 3. This plot demonstrates that most destructive from the viewpoint of the lost energy are modes where the parameter α is small.

For the typical value of the resistance $z_1 = 0.5\ \Omega$/cm and $t_r = 50$ ns, the peak current of the precursor makes up 20% of the total current through the wire array. As the current rise time is lengthened to 500 ns, the peak precursor current increases to 78% of the total wire array current.

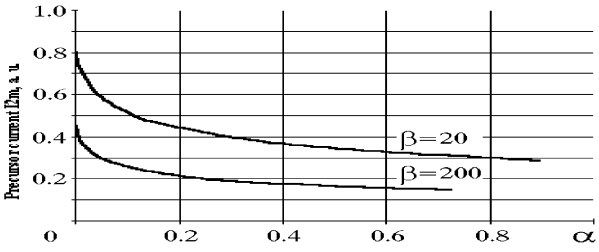

Fig. 3. The precursor peak current *versus* parameter $\alpha = \mu_0/[2\pi t_r(z_1 + z_2)]$.

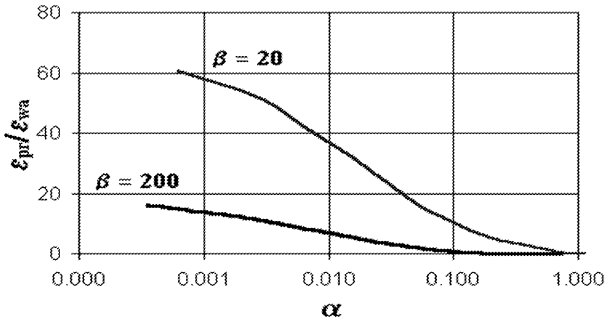

Fig. 4. Ratio of the precursor energy ϵ_{pr} to the wire array energy ϵ_{wa} as a function of $\alpha = \mu_0/[2\pi t_r(z_1 + z_2)]$ for two $\beta \propto m_{pr}^{-1}$ values.

The ratio of the precursor energy to the total energy of the wire array can be estimated using the following well-known expression for the kinetic energy of a wire array:

$$\epsilon_{wa} = \frac{1}{2} I_m^2 \ln \frac{r_0}{r_f} \approx 0.5 I_m^2 \ln 10.$$

In view of the above notations [Eqs. (5) and (6)], we obtain

$$\epsilon_{pr}/\epsilon_{wa} = \epsilon_2/\ln 10.$$

Figure 4 presents the ratio $\epsilon_{pr}/\epsilon_{wa}$ as a function of α. The plot was constructed under the assumption that the precursor was compressed 10-fold. It can be seen that even at high values of α, the precursor energy makes up a few percent of the total energy of the wire array and increases up to 50% at small α.

Precursor behavior is dependent upon the rate of rise of the wire core resistance. Let the core resistance z_1 be equal to corona resistance z_2 at the time when the precursor current peaks. In this case, the supply of the wire material to the precursor ceases. However, if the core resistance is still rather high, the supply of the wire material to a precursor will continue as observed by Lebedev *et al.* (1998).

3. WIRE ARRAY EXPERIMENTS ON THE GIT-12 SYSTEM

In this section we describe the results of experiments with a wire array performed at different current rise times and estimate the resistance of the core of an individual micron-sized wire by expressions (10)–(11).

3.1. Experimental setup

The experiments were carried out on the electrophysical complex GIT-16 (Bugaev *et al.*, 1997) generator, which currently works in 12-module configuration (GIT-12).

https://doi.org/10.1017/S026303460119302X Published online by Cambridge University Press

GIT-12 is a pulsed current generator with an intermediate inductive energy store and a plasma-opening switch (POS). Each module is composed of a primary capacitor storage, which consists of nine parallel sections assembled by the Marx generator scheme, a vacuum insulator, and a vacuum coaxial line connecting the module to the central collector. At 50-kV Marx charge voltage, the generator stores 2.56 MJ of energy. A 1.5-m-diameter central collector is supported by a high-impedance vacuum line that also serves as a part of an inductive divider for voltage measurements. The plasma-opening switch and the imploding load are placed on the top of the collector. The upstream inductance is equal to 112 nH; the downstream inductance is 55 nH. The experiments were carried out at 40-kV Marx charge voltage. The currents upstream and downstream of the POS are monitored by *B*-dot loops and inductive rings.

An additional *B*-dot loop B_1 was located inside the wire array. The distance between the axis and the B_1 loop was 1.1 cm. The implosion dynamics of the *z* pinch were recorded by a visible-light streak camera having a writing speed of 125–250 ns/cm. The streak camera inlet slit was aligned perpendicular to the *z*-pinch axis.

Tungsten and copper wire arrays were used in the experiments. The number of wires was varied from 8 to 16. The wire array length was equal to 4 cm. The wire array initial diameter was 3 cm. We used two modes of the operation of the GIT-12 generator: with the POS (nanosecond mode) and without it (microsecond mode). In the nanosecond mode, we had a current up to 2 MA with a 200-ns rise time. In the microsecond mode, we had a 1.5-MA current with an 800-ns rise time.

3.2. Experimental results and discussion

Let us first consider the qualitative difference between the implosions of a copper wire array in the nanosecond and the microsecond modes. In both cases, the wire array consisted of 16 wires; each wire had a diameter of 16 μm. The corresponding streak camera pictures and oscillograms of the current through the wire array are given in Figure 5 (nanosecond mode) and Figure 6 (microsecond mode). Here the current-derivative waveform obtained with the help of the B_1 loop placed at a radius of 1.1 cm is shown.

From the given waveforms it can be seen that the B_1 loop shows an increase in the magnetic field inside the wire array that is associated with the motion of a plasma precursor. In the nanosecond mode, the precursor current increases within 100 ns after the beginning of the increase in the current through the wire array. After the current maximum, the precursor current decreases, as predicted by the above analysis. In the microsecond mode, the precursor current goes on increasing throughout the wire array implosion. We have estimated the ratio of the precursor current I_{pr} to the total current through the wire array I_{wa}. Typical values of this ratio were equal to 0.01 for the copper wire array and 0.14 for the tungsten ones.

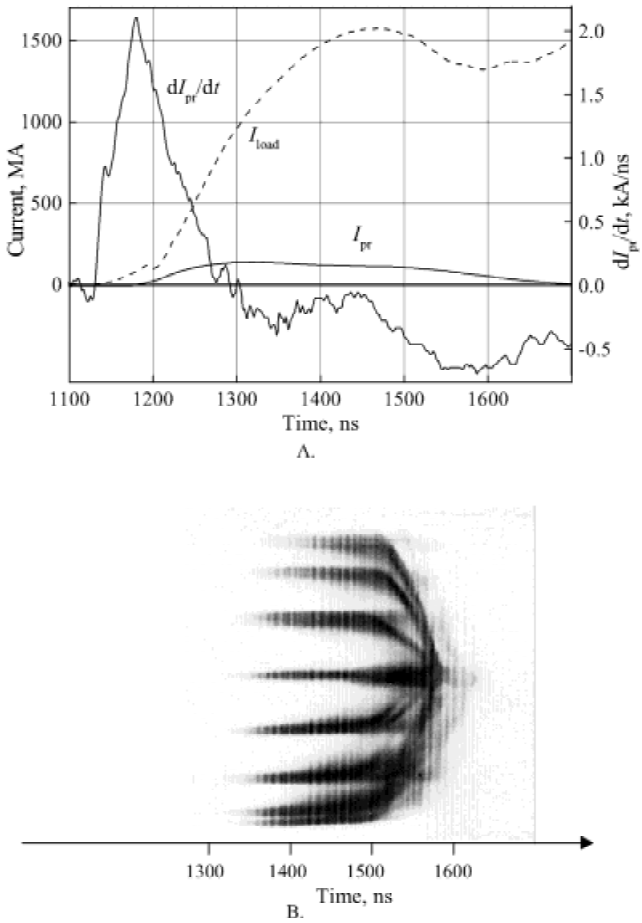

Fig. 5. A: Traces of the load current and precursor current for a copper wire array implosion (30-mm diameter, 16 wires), nanosecond mode. It can be seen that the precursor current has a maximum. B: Streak camera picture for this implosion.

Let us compare the experimental results with the predictions of the analysis given in the preceding section. We show the dependencies of I_{pr}/I_{wa} on the number of wires in the array for the copper wire arrays for the nanosecond and microsecond modes. These plots are shown in Figure 7. We would like to mention first of all that in the experiment the value of I_{pr}/I_{wa} increased in going from the nanosecond to the microsecond mode of implosion. This fact agrees qualitatively with Eqs. (10)–(11) describing the mentioned behavior of I_{pr}/I_{wa} and with the curves plotted by these equations in Figure 3, since the maximum precursor current is inversely proportional to the current rise time.

The strong dependence of the precursor current on the number of wires is also explained adequately in terms of the above analysis. Actually, the total resistance of the skeleton of a wire array is given by $z_1 = N^{-1}r_w$, where N is the number of wires in the array and r_w is the resistance of a wire. As N is increased, the quantity $\alpha = \mu_0/[2\pi t_r(z_1 + z_2)]$ should rise abruptly which is related to a decrease in resistance of the immobile part of the wire array where individual wires are connected in parallel. It is this fact that is illustrated by the data presented in Figure 7.

https://doi.org/10.1017/S026303460119302X Published online by Cambridge University Press

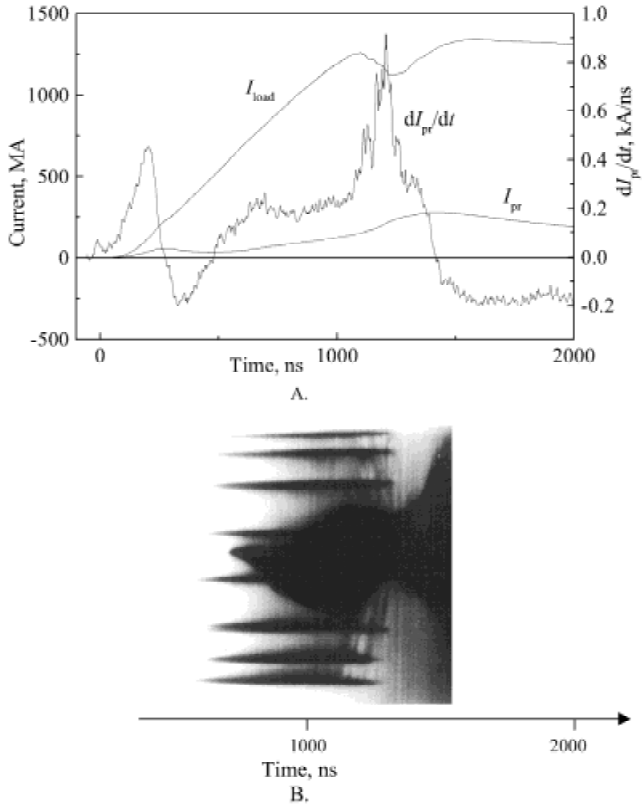

Fig. 6. A: Traces of the load current and precursor current for a copper wire array implosion (30-mm diameter, 16 wires), microsecond mode. It can be seen that the precursor current increases during all run-in phase. B: Streak camera picture for this implosion.

At the same time, the actual magnitude and waveform of the precursor current disagree with predictions. In particular, on the microsecond time scale, the measured precursor current has no maximum, as seen in the results of the calculations. This can be accounted for by the fact that for a low rate of rise of the wire array current ($dI/dt < 2 \times 10^{12}$ A/s) and a small number of wires, the precursor mass increases continuously in the process of implosion: plasma flows from individual wires forming an array are seen throughout the run-in phase. It seems that some portion of the wire array current continuously goes away with these plasma flows. Perhaps, when the distance between the wires is decreased to 1–1.5 mm, as happens in experiments on Z facility (Sanford *et al.*, 1998), the formation of a solid shell hinders the continuous plasma flow into the internal cavity of the wire array.

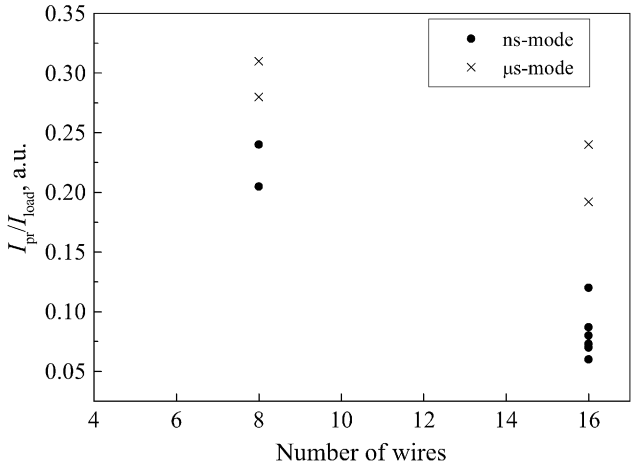

Fig. 7. Dependencies I_{pr}/I_{load} ratio *versus* the wire number for nanosecond and microsecond modes for a copper wire array.

Another experimental fact is that the measured value of I_{pr}/I_{wa} is smaller than the predicted value. It should be noted that, unfortunately, the probe placed inside the wire array becomes screened in the course of time and its readings become understated. This is indirectly evidenced by the great difference between the implosion time predicted by a 0-D simulation and that estimated experimentally. Thus, for the nanosecond mode of implosion (Fig. 5) this difference is about 100 ns, while for the microsecond implosion this difference is 400 ns.

The experimentally measured values of I_{pr}/I_{wa} allow us to estimate the core resistance for an individual wire. Actually, according to Figure 3, for 10% mass removed ($\beta = 200$) and $I_{pr}/I_{wa} = 0.35$, we have $\alpha = \mu_0/[2\pi t_r(z_1 + z_2)] = 0.05$. From this relation, we can find the resistance of the stationary part of the wire array, z_1, taking into account that $z_1 \gg z_2$. For a 16-wire array, we have the core resistance equal to about 30 Ω/cm. Using this value to determine the conductivity, we obtain about $6 \times 10^6\ \Omega^{-1}\mathrm{m}^{-1}$. According to the dependence given Bakulin *et al.* (1976), the conductivity of copper near the critical point is even lower: $10^6\ \Omega^{-1}\mathrm{m}^{-1}$. The obtained result, notwithstanding that the estimates are rather rough, correlates well with the recent experiments of Shelkovenko *et al.* (1999), where it has been shown that the core of a wire is a mixture of plasma and condensed phases.

4. CONCLUSION

We have demonstrated that the main reason for the appearance of the precursor is the high resistance of the core of an exploding wire in a wire array. The core resistance increases to 10–15 Ω within a few nanoseconds after the onset of current. Based on this information, we may describe the phenomena occurring during the formation of the precursor in a wire array as follows:

Within a few nanoseconds after the onset of current, individual wires explode, giving rise to the formation of heterogeneous pinches consisting of a high-conductivity corona and a low-resistance dense core at the sites of individual wires. According to Sarkisov *et al.* (2000), the cross-sectional area of the corona is larger than the cross-sectional area of the core by more than two orders of magnitude. In a time of the order of 10^{-8} s, almost the entire amount of the wire array current passes through the light portion of the plasma. This results in the acceleration of the corona plasma toward the wire array axis. At the same time, the bulk of the material confined in the wire core is practically stationary. With that,

https://doi.org/10.1017/S026303460119302X Published online by Cambridge University Press

the removal of the plasma corona from the core moderates the heating of the latter that generally occurs due to electronic and radiation heat transfer during the explosion of an individual wire without the effect of a magnetic field from the neighbor wires of the wire array.

The motion of the corona plasma toward the center leads in turn to an increase in dL/dt and a related increase in voltage across the core and, hence, to an increase in the energy delivered to the core. As a result, the corona formation process will repeat again and again and the precursor plasma will go by discrete portions toward the wire array center. The gradual removal of the plasma will result in a decrease in core mass, and in the end all of the substance of the wire core will go over to the plasma state. The plasma columns formed on the site of the exploded micro wires will be homogeneous, that is the region of dense material with a high resistance inside the plasma columns will disappear. It should be noted that an increase in the number of wires in an array not changing its mass will result in a decrease in the diameter of an individual wire. Owing to this, the lifetime of the precursor will decrease abruptly due to the fact that the core will disappear within a shorter time.

Thus, the process of precursor formation described above results in somewhat longer implosion times. As this takes place, the total energy balance varies only weakly provided the wire array implodes on the nanosecond time scale.

ACKNOWLEDGMENTS

This work was partly supported by Project 525 of ISTC. The authors appreciate the help of their colleagues F. Fursov, N. Kurmaev, and Yu. Labetsky.

REFERENCES

Aivazov, I.K. *et al.* (1987). *Pis'ma v Zh. Eksp. Teor. Fiz.* [*JETP Lett.*] **45**, 23.
Baksht, R.B. *et al.* (1983). *Fiz. Plasmy* [*Sov. J. Plasma Phys.*] **9**, 706.
Baksht, R.B. *et al.* (1989). *AIP Conf. Proc.*, no. 195, 27.
Bakulin Yu.D. *et al.* (1976). *Sov. Phys. Tech. Phys.* **20**.
Bugaev, S.P. *et al.* (1997). *Izv. Vyssh. Uchebn. Zaved. Fiz.* [*Sov. Phys. J.*], **40**, 38.
Haines, M.G. (1998). *IEEE Trans. Plasma Sci.* **26**, 1275.
Lebedev, S.V. *et al.* (1998). *Phys. Rev. Lett.* **81**, 4152.
Ratachin, N.A. & Baksht, R.B. (2001). *IEEE Trans. Plasma Sci.*, in press.
Sanford, T.W.L. *et al.* (1998). *IEEE Trans. Plasma Sci.* **26**, 1086.
Sarkisov, G. *et al.* (2000). *Bull. Am. Phys. Soc.* **45**.
Shelkovenko, T.A. *et al.* (1999). *Rev. Sci. Instrum.* **69**, 1999.
Zakharov, S.M. *et al.* (1983). *Fiz. Plazmy* [*Sov. J. Plasma Phys.*] **9**, 469.